

Experimental Study and Design Evaluation of Impingement Steam Jet

F. Masuda, T. Nakatogawa

*Plant Engineering Department,
Mitsubishi Atomic Power Industries, Inc., Engineering Center,
2-1, Taito 1-chome, Taito-ku, Tokyo 110, Japan*

K. Kawanishi, M. Isono

*Takasago Technical Institute,
Mitsubishi Heavy Industries, Ltd., Shinhama,
2-chome, Arai-cho, Takasago, Hyogo, Japan*

SUMMARY

The experimental study on impingement steam jet to develop the evaluation method in the design against the postulated pipe rupture was performed. In this time, the experiments have been carried out to obtain more detailed data and to more clarify the characteristics than that in the previous paper F6/2 of 5th SMiRT.

The stagnant steam conditions are steady-state saturated and pressure range is 2.06 ~ 4.56MPa, and the employed nozzle shapes are circle(short pipe) and ellipse(opened in longitudinal side of the pipe) simulating the break geometry postulated in the design.

The data about thrust forces, impingement forces, impingement pressure profiles and so on were obtained. Particularly about the pressure profiles, a number of detailed data were obtained at various impingement distances over the wide axial range. In the case of jet from an elliptical nozzle, it was found that the expansion on minor axis of the nozzle is remarkably greater than that on major axis, particularly near the nozzle exit.

Reflecting experimental data, evaluation model of jet impingement effects applied to design were derived with reference to that of ANSI-N176.

1. Introduction

In the design of nuclear power plant, it is required to secure the safety of plant against the effects caused by jet flow under the postulated pipe rupture accident. There are thrust forces, impingement loads, environmental effects and so on in those effects. They have a serious effect on the structural design of the building, equipments and the other components. For thrust forces and environmental effects, fairly enough information or understanding seem to have been obtained. On the other hand, for the characteristics of high energy jet, the study has not been enough until now to establish applicable evaluation methods in the design. Particularly, there are many unknown characteristics of jet in the case of high energy fluid conditions such as high pressure steam attending the highly-under-expanded condition or subcooled water behaving as two phase jet, including effects of nozzle geometry supposed in the design.

From this point of view, the experimental study has been carried out to clarify the characteristics of jet and its effects. In the previous study, the fundamental experimental study on subcooled water and steam jet has been carried out and the results of them were reported in the paper F6/2_of 5th SMIRT.^[1] In this time, the experimental study of impingement steam jet was carried out to obtain more detailed data and to more clarify the characteristics over the wide axial range including the effects of nozzle geometry.

In this paper, the main results of the experiment of impingement steam jet and evaluation model of jet impingement effects applied to design are described.

2. Experimental apparatus and procedure

A scheme of experimental apparatus is shown in Fig. 1. Steam jet is ejected downward into the atmospheric environment and vertically impinges on the flat plate. Nozzle reaction force is measured by the load cell contacted with the nozzle. Impingement force and impingement pressure distribution are measured by the load cells and pressure gauge attached to the impingement plate. Impingement plate is designed to be movable horizontally and vertically to enable the measurements of axial variation of impingement forces and pressure distributions.

As shown in Fig. 2, two types of nozzle are employed. One is circle (short pipe) and the other is ellipse opened in the longitudinal side of pipe simulating the break geometry of which aspect ratio is 4, postulated in the design. For surveying the effect of flow contraction, two type edge entrances which are round and sharp are provided with each nozzle type.

The stagnant steam conditions are steady-state dry saturated, and pressure range is 2.06 ~ 4.56 MPa.

3. Experimental results and discussion

3.1 Nozzle reaction and impingement force

Measured nozzle reaction forces are plotted in Fig. 3 for the circular nozzles and in Fig. 4 for the elliptical nozzles. Differences were not seen practically between the impingement force data and nozzle reaction force data. These forces are defined as

$$F_R = F_j = K \cdot (P_0 - P_\infty) \cdot A_e \quad (1)$$

where F_R : nozzle reaction P_0 : initial stagnation pressure
 F_j : impingement force P_∞ : environmental pressure (=101.3KPa)
 K : thrust coefficient A_e : discharge area

From eq. (1) with the experimental data, thrust coefficient K are obtained as followings,

$K = 1.21$ for the circular nozzle with round edge
 $= 1.12$ for the circular nozzle with sharp edge
 $= 1.14$ for the elliptical nozzle with round edge
 $= 1.08$ for the elliptical nozzle with sharp edge

These values is smaller than $K=1.24$ which is obtained from Moody's critical flow model for the ideal nozzle.^[2] K value of sharp edge is relatively smaller than that of round edge, it shows that the flow contraction causes the reduction of reaction and impingement forces. And K value of ellipse is relatively smaller than that of circle, it may show that pressure drop of upstream to the exit and contraction effect at the exit cause the reduction of forces.

Variation of impingement forces and central stagnation pressure on the plate in short distances $H/D = 0.01 \sim 0.5$ were measured for the circular nozzle. As shown in Fig. 5, impingement forces and pressures increase with decreasing of distance. It is attributed to that the sonic plane moves from nozzle exit to the gap between nozzle lip and the plate surface and the high pressure region on the plate surface increases.

3.2 Characteristics of impingement pressure distribution

From point of application to the design evaluation, it is required to seize various characteristics of impingement jet in consideration of the initial fluid condition, nozzle geometry, impingement distance, impinged target geometry or inclination, ambient pressure and so on.

In this time, the basic experiments have been carried out in order to seize the characteristics of impingement high pressure steam jet to clarify the effects of initial stagnant pressure, impingement distance and nozzle geometry. The pressure distributions were measured at the impingement distance $H/D = 0.5 \sim 62.5$ for the circular nozzle and $H = 5 \sim 373\text{mm}$ for the elliptical nozzle (major dia. $\approx 20\text{mm}$, minor dia. $\approx 5\text{mm}$).

3.2.1 Characteristics of impingement jet from the circular nozzle

Typical structures of highly under-expanded free and impingement jet from the circular nozzle are shown in Fig. 6. In figuring, the schlieren photographs in Kukita's study^[3] were referenced.

An example of the measured impingement pressure distributions for $P_0 = 4.02\text{MPa}$ and some examples of variation of central pressure are shown in Fig. 7 and Fig. 8. These are roughly divided into following three regions on jet axis according to the characteristic of distribution.

1) First region: In the region near the nozzle exit, the rapid expansion attended with reduction of impingement pressure occurs and the pressure profile changes from smooth type to the type which has the shoulders. Increasing the distance further, the central peak falls and the flat pattern occurs. The location where the flat pattern is formed seems to be approximately equal to the location of mach disk referencing Love(et al.)'s study^[4]. (Though the location of mach disk in Love's study is for air jet, the differences of characteristics between steam and air is

expected to be small.) Considering that the detached shock wave is formed in front of the plate in this first region, variation of central pressure is approximately expressed by the normal shock wave relation for stagnation pressure ratio across the shock wave.

The calculated result with the normal shock wave relation is shown in Fig. 8 as the broken line. (In calculations, Owen(et al.)'s study^[5] were referenced.) Slight shift of the experimental data may be attributed to that the shock wave is formed in front of the plate.

2) Second region: Remarkable radial expansion does not occur in this region. But, as the central pressure reduces with an increase of the impingement distance, the pressure profile changes from the flat type to the concave (like the saddle-back) type. Then the recovery of pressure occurs in the center with an increase of the impingement distance and a re-transition of the pattern from the flat type to the smooth type is seen. The end of the second region may be defined as the point where the maximum recovery pressure occurs. As shown in Fig. 8, the distance at which the bottom pressure occurs is equal to about 2.5 times of that of the mach disk, and the distance at which the maximum recovery pressure occurs is equal to about 5 times of that of the mach disk. The bottom pressure and the maximum recovery pressure increase slightly with the decrease of the initial stagnation pressure. In addition to the above, it is seen that the bottom pressure is approximately equal to that calculated in the normal shock wave relation at the mach disk location. Then it is considered that the characteristics of impingement jet in this region is remarkably affected with mach disk location in the jet.

3) Third region: In this region, jet expands gradually and the central pressure monotonously decays with the growth of the mixing region. As well known, the characteristics of the impingement pressure distribution is given by the half-width expression once the mixing region is fully developed. Referencing Fig. 8, the distance for the beginning of the turbulent jet is equal to about 10 times of that of the mach disk.

3.2.2 Characteristics of impingement jet from the elliptical nozzle

Up to the present, enough theoretical or experimental study on the highly under-expanded jet discharged from the nonaxisymmetric nozzle, such as the ellipse in this study, has not been found.

An example of the impingement pressure distributions along the nozzle axis are individually shown in Fig. 9(a) and 9(b) for $P_o = 4.56\text{MPa}$. Examples of variations of central pressures are shown in Fig. 10. As well as to the case of the circular nozzle, these are roughly divided into three regions on jet axis according to the characteristic of distribution. However, following some particular characteristics seem to exist.

- 1) The expansion along the minor axis is greater than that along the major axis in the measured region. This tendency is remarkable in the region near the nozzle exit.
- 2) Concerning to the distance of transitional points where the type of pressure profile changes, the test results of measurements show that the transition on the minor axis occurs at nearer distance than that on the major axis.

4. Examinations of evaluation models for the design

As one of developments of impingement jet evaluation models for the design, the examinations employing the method of the ANSI-NL76 model^[7], which is of three regions, were performed. As a result of examinations, it was found that the ANSI-NL76 model gives considerably larger impingement pressure and less expansion than those of the experimental data in the first and second region of jets for the circular nozzle, besides for the elliptical nozzle, the ANSI-NL76 does not fairly match with experimental results.

Thus, the following modifications of the ANSI-NL76 model was proposed.

- 1) For the circular nozzle, the expansional half-angle in the first region is defined as ϕ' which is given by multiplying coefficient λ into ϕ defined in the ANSI-NL76 model. As an appropriate value, $\lambda=2.0$ was obtained from the pressure profiles of the experimental data.
- 2) For the elliptical nozzle, as appropriate values, $\lambda=2.0$ on minor axis and 0.0 (non-expansion) on major axis in the first region were obtained from the pressure profiles of the experimental data. Besides, in the third region expansional half-angle 30° on minor axis and 5° on major axis in opposed to uniform 10° of the ANSI-NL76 model were obtained from the pressure profiles of the experimental data.

5. Conclusions

Principal results in this study are followings.

- (1) Thrust coefficient K values for each nozzle types were obtained from measurements of nozzle reaction forces and impingement forces. Comparing these values with 1.24 obtained theoretically from applying Moody's critical flow model, thrust coefficient for only the circular nozzle with round edge entrance is practically equal, and for other nozzle types substantial reduction exists.
- (2) Impingement forces in the region near the nozzle exit ($H/D = 0.01 \sim 0.5$) for the circular nozzle were also measured. It was found that impingement forces in this region were greater than those in further region on the jet axis.
- (3) For both cases of the circular and elliptical nozzle, pattern of impingement pressure distribution of jet remarkably changes with the increase of the impingement distances and jet is roughly divided into three regions.
- (4) For a circular jet, the impingement distances where the pattern of distribution changes distinctly depends on the location of mach disk which is determined by the initial stagnant pressure.
- (5) For an elliptical jet, the expansion on minor axis is remarkably greater than that on major axis, particularly near the nozzle exit. The impingement distance where pattern of distribution changes distinctly depends on the initial stagnant pressure as well as the case of the circular nozzle. However, the distance of transitional points where the type of pattern changes on minor axis is slightly shorter than that on major axis.
- (6) As one of developments of impingement jet evaluation model for the design, examinations employing the method of the ANSI-NL76 model were performed, some modifications for that model were proposed in order to obtain a substantial agreement with experimental results.

6. References

1. Kitade, K., et al., "Experimental study of pipe reaction force and jet impingement load at the break" paper F6/2 of 5th SMIRT, Berlin, August 1979.
2. Moody, F. J., "Maximum Flow Rate of a Single Component Two-Phase Mixture" Journal of Heat Transfer, ASME, Series C, Vol. 87, 1965.
3. Kukita, Y., "Study on unstable phenomena of supersonic impinging jets" Ph. D. Thesis, University of Tokyo, December, 1974.
4. Love, E. S., et al., "Experimental and theoretical studies of Axisymmetric free jets" NASA Technical report R-6, 1959.
5. Owen, P. L., et al., "The Flow in an Axially-Symmetric Supersonic Jet from a Neary Sonic Orifices into a Vacuum" Brit., A. R. C. Technical Report, R&M 2616 (1952).
6. Donaldson, C. D., et al., "A study of free jet impingement. Part 1. Mean properties of free and impinging jets" J. Fluid Mech., Vol. 45, part 2, 1971.
7. ANS, "ANSI N176 - Design Basis for Protection of Nuclear Power Plants against Effects of Postulated Pipe Rupture" December, 1979.

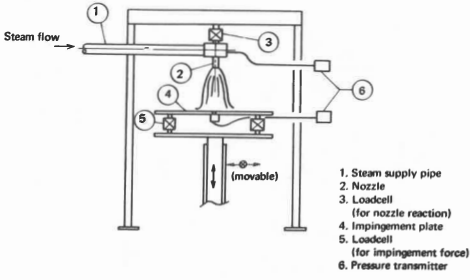


Fig. 1 Sketch of experimental apparatus

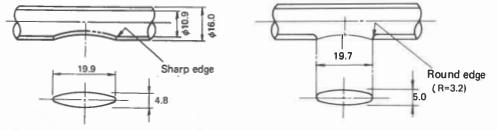
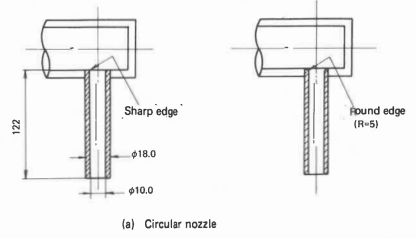


Fig. 2 Nozzle geometry

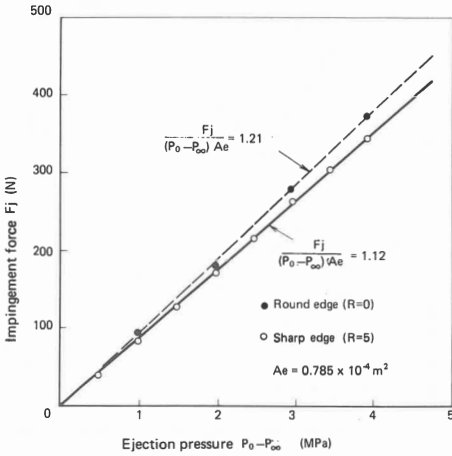


Fig. 3 Impingement jet forces for the circular nozzle

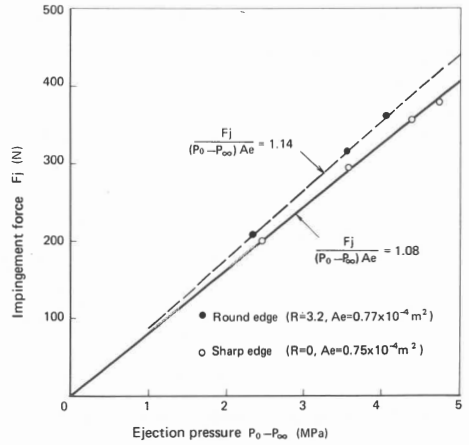


Fig. 4 Impingement jet forces for the elliptical nozzle

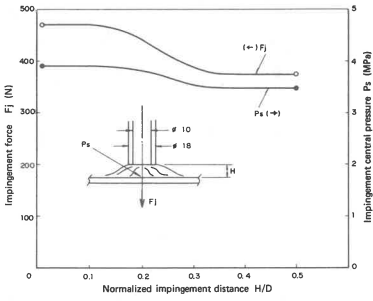
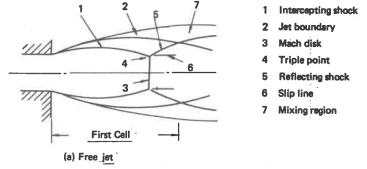
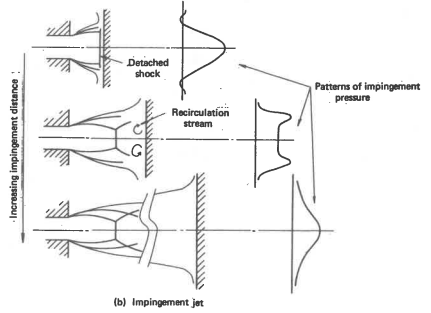


Fig. 5 Impingement jet forces and central pressures at short distances (Circular nozzle $R=5$, $P_0 - P_{atm} = 3.92$ MPa)



(e) Free jet



(b) Impingement jet

Fig. 6 Structure of highly under-expanded jet

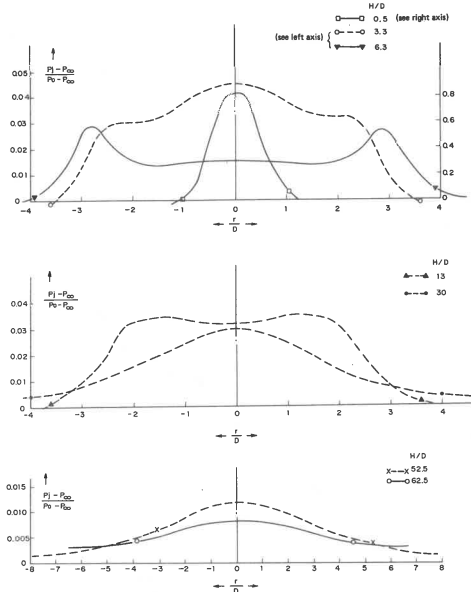


Fig. 7 Impingement pressure profiles ($P_0 = 4.02$ MPa, circular nozzle with sharp edge entrance)

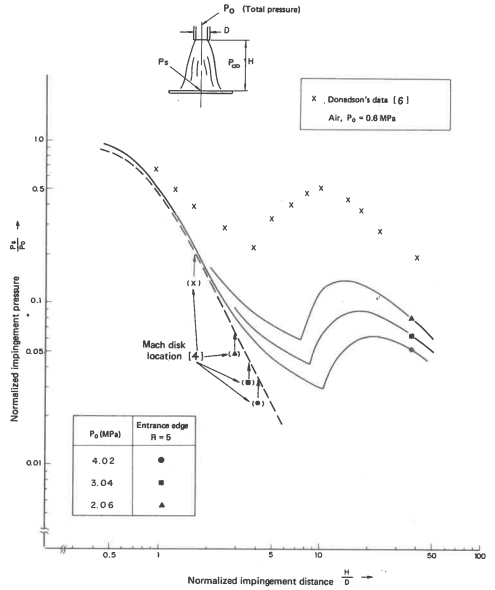


Fig. 8 Variation of central impingement pressure for the circular nozzle

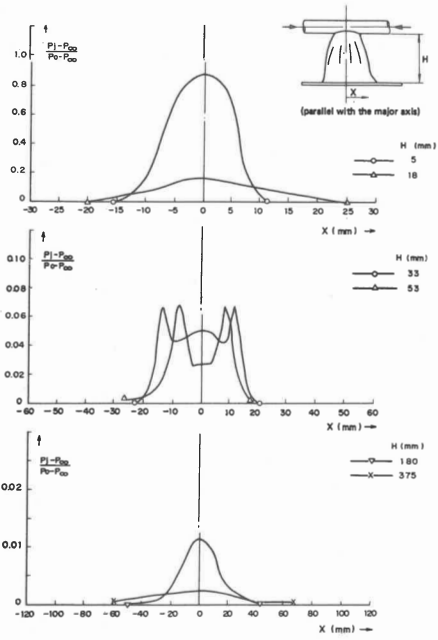


Fig. 9 (a) Impingement pressure profiles for the elliptical nozzle ($R=0$, $P_0=4.56$ MPa, X direction)

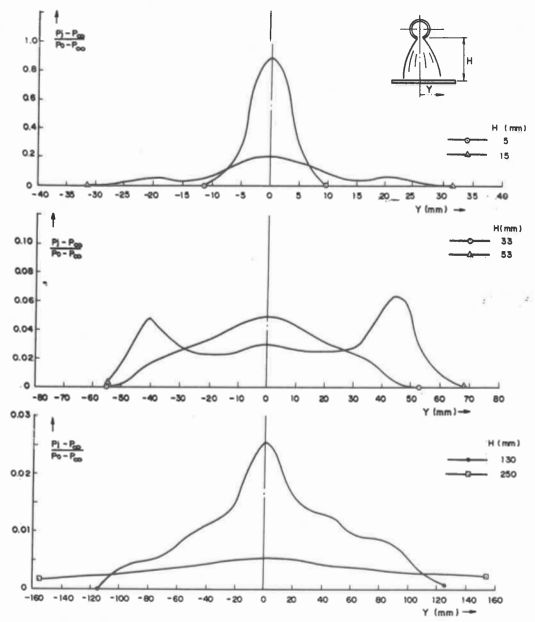


Fig. 9 (b) Impingement pressure profiles for the elliptical nozzle ($R=0$, $P_0=4.56$ MPa, Y direction)

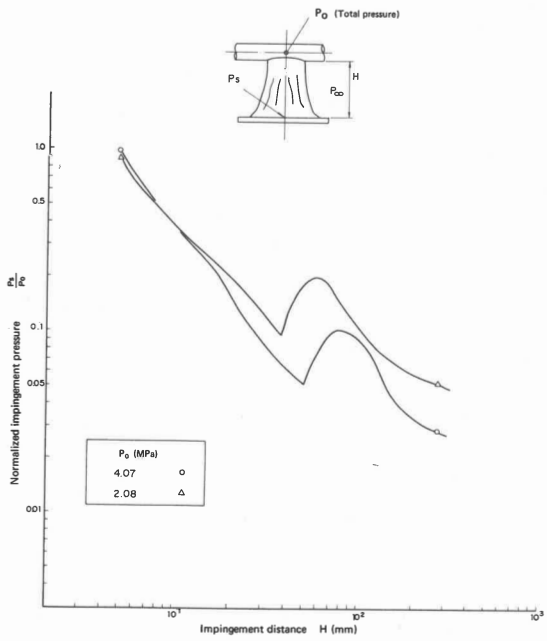


Fig. 10 Variation of central impingement pressure for the elliptical nozzle

